

THREE-DIMENSIONAL FINITE ELEMENT ANALYSIS OF OSSEOINTEGRATED DENTAL IMPLANTS

Luigi Baggi¹, Ilaria Cappelloni², Franco Maceri², Giuseppe Vairo²

¹University of Rome “Tor Vergata”, School of Dentistry
00133 Roma, via Montpellier 1, Roma, Italy

²University of Rome “Tor Vergata”, School of Medical Engineering
00133 Roma, via del Politecnico 1, Roma, Italy

vairo@ing.uniroma2.it (Giuseppe Vairo)

Abstract

In this paper the biomechanical interaction between osseointegrated dental implants and bone is investigated by numerical simulations. The influence of some mechanical and geometrical parameters on bone stress distributions is highlighted and some risk-measures relevant to critical overloading are furnished. Load transfer mechanisms of several dental implants are analyzed by means of linearly elastic finite-element analyses, when static functional loads occur. For a given implant the variation of its performance with the placement is investigated, considering insertions both in mandibular and maxillary molar segments. The mechanical properties of the bone regions (cortical and cancellous) are approximated with those of a type II bone and the geometry of crestal bone loss after a healing period is modelled. Five commercially-available dental implants are analyzed, demonstrating as the optimal choice of an endosseous implant is strongly affected by a number of shape parameters as well as by anatomy and mechanical properties of the site of placement. Numerical results clearly proof as a given implant device exhibits very different performance on mandibular or maxillary bone segments, resulting in higher compressive stresses when maxillary placement is experienced. Finally, the effectiveness of several multiple-implant restorative applications is investigated. The first one is related to a partially edentulous arch restoration, based on a double-implant device involving a retaining bar. Other applications regard single-tooth restorations based on non-conventional devices consisting in a mini-bar supported by two mini endosteal implants, possibly reproducing the natural roots orientation of a multiple-root tooth.

Keywords: dental biomechanics, osseointegrated implants, finite-element analysis.

Presenting Author's Biography

Giuseppe Vairo. Born 1974, he achieved his Mechanical Engineering degree cum laude in 1998 and PhD degree in Structural Mechanics in 2002 at University of Rome “Tor Vergata”, Italy. From 2004 he is Assistant Professor of Structural Engineering at the Department of Civil Engineering, University of Rome “Tor Vergata”. Main fields of interest are: finite-element structural analysis, mechanics of composite structures, wind-structure interaction, long-span bridges, dental biomechanics, vascular stent analysis.



1 Introduction

Osseointegrated dental implant represents one of the main treatments for restoring completely or partially edentulous patients and its success is strictly related to the direct connection between living bone and the surface of a load-bearing artificial structure, generally titanium-based. Endosteal implants can be usually employed to support a single-tooth prosthesis or fixed partial denture. In this latter occurrence multiple-implant systems are generally involved and a number of screws supports the denture prosthesis by means of devices such as retaining bars, retaining balls, natural-like bridges.

As confirmed by several clinical studies [1–3], osseointegrated implants can fail essentially as a consequence of bone weakening or loss at the peri-implant region. This occurrence can be induced by surgical trauma or bacterial infection as well as by overloading of the living tissues. Therefore, premature implant use, incorrect prosthesis and implant design, improper surgical placement, can activate bone resorption processes as a consequence of high stress concentrations at the peri-implant tissues. Accordingly, an accurate evaluation of the bone stress distribution under functional loads allows to investigate about the effectiveness and reliability of endosseous implants, highlighting possible failure risks [4, 5].

Stress fields around osseointegrated dental implants are affected by a number of biomechanical factors: geometry and typology of implant devices [6–8], implant and bone mechanical properties [9–11], patient's physiological conditions [12, 13], geometry of the site of insertion [14–16]. As far as the implant shape is concerned, design parameters that mainly affect the load transfer characteristics, that is the stress/strain distribution in the bone, include the implant diameter and the length of the bone-implant interface, as well as thread pitch, shape and depth, when threaded implants are considered. Threaded implants are generally preferred to smooth cylindrical ones, in order to increase the connection surface of the implant [17]. Depending on bone quality, surface treatments and thread geometry can significantly influence the implant effectiveness, in terms of both primary implant stability and biomechanical nature of the bone-implant interface after the healing process [6, 18].

Despite the number of researches in this field, stress analysis on implant-bone interfaces yet represents an open task, because of the wide range of implant applications and implant typologies. Nevertheless, the complex geometry of the coupled biomechanical bone-implant system prevents the use of a closed-form approach for stress/strain evaluation and then numerical methods are usually employed. In last years, the finite-element method [19] has been widely used in applied dentistry for analyzing both restorative techniques [20–23] and implant applications [24, 25], investigating the influence of implant and prosthesis designs [7, 8, 26–29], of magnitude and direction of loads [28–31], of bone mechanical properties [11, 32] as well as model-

ling different clinical scenarios [13, 32–35].

In this paper a number of endosteal implant applications are analyzed by means of static three-dimensional linearly elastic finite-element simulations. In detail, firstly five commercially available osseointegrated dental implants are numerically investigated, highlighting the biomechanical interaction between implant system and bone as well as the influence of some mechanical and geometrical parameters on load transfer mechanisms and on bone stress distributions. In order to investigate how the intervention site affects the implant performance, insertions both in mandibular and maxillary molar segments are considered. In agreement with the clinical evidence after a healing period [36, 37], different compact bone geometries around the implant neck are modelled, depending on the crestal bone loss induced by implant shape.

Afterwards, three implant applications based on multiple-implant systems are analyzed, considering mandibular insertions. The first one is related to the case of partially edentulous arch restoration and it is based on a double-implant device involving a retaining bar, that is a gold alloy bar supporting the prosthetic denture, fixed to two endosteal implants [38]. It will be denoted in the sequel as DIRB. The other two applications regard the case of single-tooth restorations based on a non-conventional device. It will be denoted as MI and consists in a mini-bar (titanium-based) which is supported by two mini endosteal implants. These latter can be suitably angled (two cases are numerically investigated) in order to reproduce natural roots orientation in multi-root teeth.

It is worth observing that the use of mini-screw implants is usually related to clinical orthodontic or skeletal applications, when temporary but absolute anchorages should be involved [39] without complete osseous integration. Therefore, the use of mini osseointegrated implants for prosthetic applications can be considered as a novel therapeutic concept. In detail, using two small screws instead of a greater one (in terms of both insertion length and diameter) should be advantageous when geometrical configuration of the site of insertion and/or bone quantity and quality (particularly in sinus zone) do not allow to employ traditional implants ensuring long-term success and/or an effective healing process. Some analyses of implants with reduced dimensions employed for prosthetic dentistry applications are available in the specialized literature [40, 41], but geometrical parameters of these smaller implants do not significantly differ from the "traditional" ones, resulting not in agreement with typical mini-screws dimensions (thread diameter ranging from 1.2 up to 2.5 mm; insertion length from 4.0 to 12 mm [42–45]).

2 Material and methods

2.1 3D numerical models

In this paper five commercial threaded dental implants are investigated (see Fig. 1):

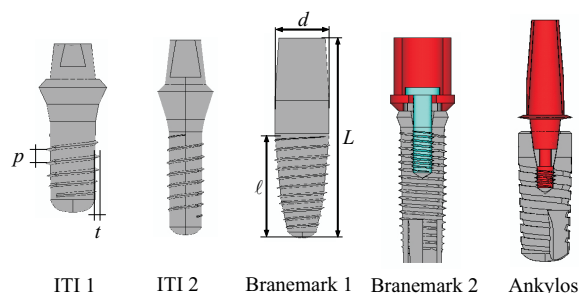


Fig. 1 Three-dimensional solid models of five commercial endosteal dental implants analyzed in this paper.

- two ITI implants (Institute Straumann AG, Waldenburg, Switzerland);
- two Branemark implant systems (Nobel Biocare AB, Goteborg, Sweden);
- an Ankylos implant system (Degussa Dental, Hanau-Wolfgang, Germany).

As sketched in Fig. 1, ITI devices and the first Branemark implant are modelled by a one-body structure; the fixture of the second Branemark implant is connected to the abutment by an internal screw; Ankylos system has a threaded abutment directly inserted on the fixture. Moreover, thread is trapezoidal for the Ankylos implant and triangular for all the other devices.

With reference to the notation introduced in Fig. 1 and as summarized in Table 1, fixture diameters and lengths of implant-bone interfaces vary between 3.3 mm and 4.5 mm, 7.5 mm and 12 mm, respectively. Furthermore, all the analyzed implants are substantially comparable in thread pitch and depth.

Three-dimensional solid models of implants and abutments are built up from high-resolution pictures and real devices. Starting from the model of the Ankylos device, solid models of multi-implant applications are also obtained (see Fig. 2). In detail, a double-implant system (DIRB) able to support three molar prosthetic crowns is modelled considering a gold retaining bar, with a length of about 22 mm, perfectly fixed to two parallel (i.e., orthogonal to the retaining bar) commercial Ankylos implants, whose interaxis is 18 mm. Moreover, non conventional single-tooth implant models are also built up (MI). In this case two mini-screws, characterized by the Ankylos geometry and whose main geometrical parameters are indicated in Table 1, are connected by a titanium-based mini-bar, whose length is 8 mm. Two different models are considered. In the first one the Ankylos-type mini-implants are assumed to be parallel (MI₀) and with an interaxis of 6 mm, whereas in the second case they are symmetrically angled at 25° (MI₂₅) with reference to the vertical axis (i.e., to the axis orthogonal to the bar). It is worth observing that the proposed mini-implants are not commercially available and they are assumed with an Ankylos-type shape in order to ensure an optimal osseous integration process (see Fig. 3).

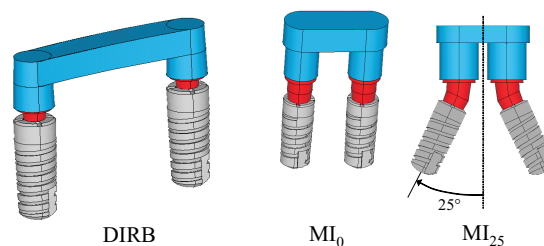


Fig. 2 Three-dimensional solid models of multi-implant devices based on Ankylos-type screws: a double-implant system with a gold retaining bar (DIRB) and two non-conventional mini-implant devices (MI).

Tab. 1 Main geometrical parameters, expressed in mm, of the implants considered in this study. Notation refers to Fig. 1: L is the implant total length; l represents the bone-implant interfacial length; d indicates the implant maximum diameter; p is the average thread pitch; t is the average thread depth.

Implant System	L	l	d	p	t
ITI1	16	7.5	4.1	1.15	0.24
ITI2	17	9	3.3	0.98	0.20
Branemark1	16	9	4.5	0.73	0.21
Branemark2	14	12	3.75	0.60	0.27
Ankylos	11	11	4.5	1.06	0.20
Mini-Ankylos	6	6	2.5	0.90	0.18

Maxillary and mandibular bone segments relevant to molar regions are modelled from CAT images, evaluating the physiological geometrical parameters of cancellous and compact bone by SimPlant[®] software. Moreover, depending on the implant shape and in accordance with the clinical evidence after the healing process, different compact bone geometries around the implant neck are considered [36, 37]. In detail, as showed in Fig. 3, for ITI and Branemark implants a “flared” shape is modelled in order to take into account a crestal bone loss of about 0.8–0.9 mm, whereas for the Ankylos device (both commercial and mini-screw type) no crestal bone loss is considered and the cortical bone follows the neck profile of the implant system (platform switching).

Bone segments (see Fig. 4) are composed by two volumes: an outer shell with an average thickness of 2 mm, representing the cortical bone layer, and an inner volume representing the cancellous bone tissue connected with the cortical’s one. Length of bone segments along mesial–distal direction (y axis in Fig. 4) is about 40 mm for single-tooth implant systems and 60 mm for the DIRB device, whereas their average height is about 16 mm for the maxillary segment and 24 mm for the mandibular one. Implant systems are assumed to be approximately placed at the midspan of bone segments.

All 3D solid models (bone segments and implants) are generated by means of a homemade preprocessing tool

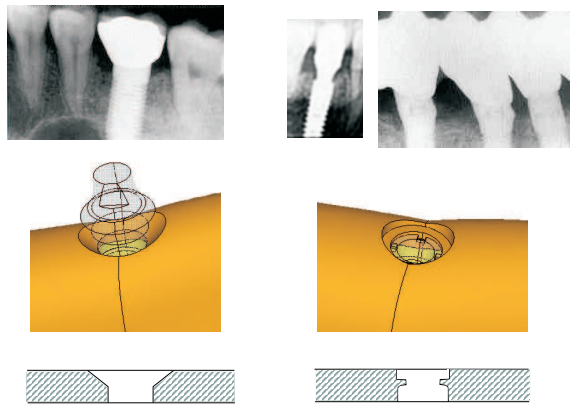


Fig. 3 Geometrical modelling of crestal bone loss induced by implant shape. Periapical radiographs and bone solid models relevant to a “flared” crestal bone loss after a healing period (on the left) and to implants inducing very reduced crestal bone loss (on the right).

developed in MatLab[®] language, able to produce primary topology of each model and whose output is fully compatible with the ANSYS[®] environment. The commercial tool ANSYS 7.1 is used for merging all the parts comprising the overall bone–implant model and for generating and solving the relevant discrete finite–element meshes. Ten–nodes tetrahedral elements with quadratic displacements shape functions and three degrees of freedom per node are employed and, as a result of preliminary convergence analyses, mean mesh–size is about 0.6 mm away from the bone–implant interface and 0.1 mm at the peri–implant regions.

2.2 Material properties

All the involved materials are assumed with a linearly elastic and isotropic behaviour and the different material volumes are considered as homogeneous. Table 2 summarizes the elastic properties used in this study. Implants, abutments and the mini–bar of MI devices are assumed to be constituted by a titanium alloy, Ti6Al4V, whereas the retaining bar of the DIRB system is modelled through a gold alloy. It is worth observing that the values of the Young’s modulus and Poisson’s ratio employed for cortical and cancellous bone approximate a type II bone quality [47].

Complete osseous integration between implants and natural tissues is assumed, enforcing as a displacement constraint the continuity of the displacement field at the implant–bone interface. Furthermore, displacement continuity is imposed between each component comprising implant systems.

2.3 Loading conditions

Finite–element simulations for the five commercial single–tooth implants are carried out considering a functional load applied at the top of the abutment without any eccentricity with respect to the vertical axis (z in Fig. 4), and angled at about 22° with reference to z . The lateral component of the force along buccal–lingual axis (opposed to the x axis direction, see Fig. 4) is as-

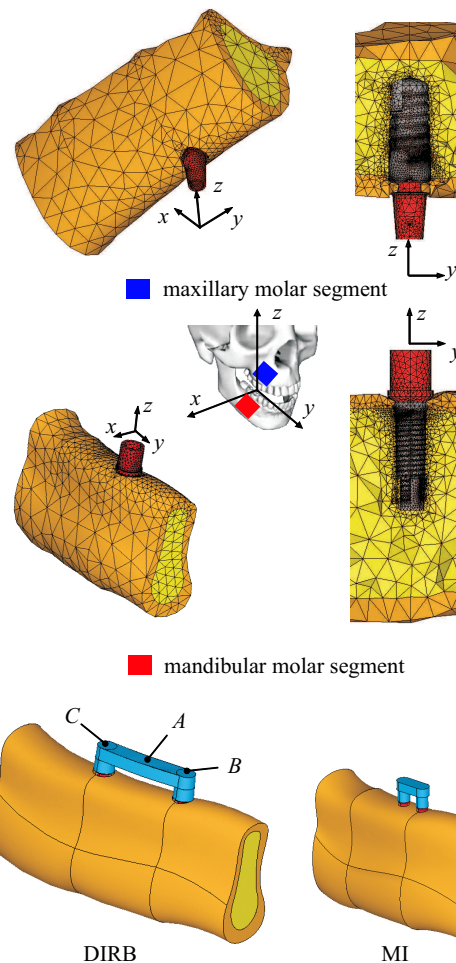


Fig. 4 Overall bone–implant models for both maxillary and mandibular bone segments. Notations and some discretized details.

sumed equal to 100 N and the vertical intrusive one is 250 N. This load is also considered in the case of DIRB and MI applications. For the non–conventional mini–screw systems (MI) the force is applied at the middle of the mini–bar, whereas when the DIRB system is experienced three different loading positions are considered on the upper–side centerline of the bar: at the midspan (position A in Fig. 4) and at the mesial and distal implant locations (positions B and C, respectively).

In order to allow significant comparisons, implant abutments and bar–implant connections are adjusted in such a way that all the loading locations are 7 mm far from the insertion bone surface.

2.4 Stress measures

For all the analyzed bone–implant systems, stress distributions are numerically evaluated on both compact and cancellous bone at the peri–implant regions, giving risk–measures of critical overloading.

Von Mises stress field σ_{VM} is used as a global stress measure for characterizing load transfer mechanisms on a given implant or device, whereas principal stresses

Tab. 2 Elastic constants adopted for FE analyses. E is the Young's modulus (in GPa) and ν is the Poisson's ratio.

Material	Zone	E	ν
Ti6Al4V	implants abutments mini-bar (MI)	114.0 ^{a,b}	0.34 ^{a,b}
Gold alloy	retaining bar (DIRB)	105.0 ^c	0.23 ^c
Cancellous bone	maxillary	0.5 ^d	0.30 ^d
	mandibular	1.0 ^a	0.30 ^d
Cortical bone	maxillary and mandibular	13.7 ^{a,e}	0.30 ^d

^a From Bozkaya et al. (2002) [30].

^b From Lemon and Dietsch-Misch (1999) [46].

^c From Natali et al. (2006) [48].

^d From Chun et al. (2005) [34].

^e From Van Oosterwyck et al. (1998) [49].

(σ_i , with $i = 1, 2, 3$) are locally employed as a risk measure of bone–implant interface failure or of resorption process activation. Assuming as a physiological limit that overloading states occur when ultimate strength of the bone is reached, maximum principal compressive and tensile stresses on the cortical bone should be less than 170–190 MPa and 100–130 MPa [50, 51], respectively, whereas the normal stresses on the trabecular bone (both in compression and tension) should be less than about 5 MPa [50].

With the aim to define quantitative stress measures useful for comparison analyses and with reference to the sketch showed in Fig. 5, let Ω_t and Ω_c be thin volumes with an average thickness of about 0.5 mm around a given implant and relevant to the trabecular and cortical regions, respectively. Let $\Sigma_t(z)$ be the two-dimensional region resulting from the intersection at a given value of the z coordinate between Ω_t and a plane orthogonal to the implant axis (which is different from the axis z when DIRB and MI devices are considered). Moreover,

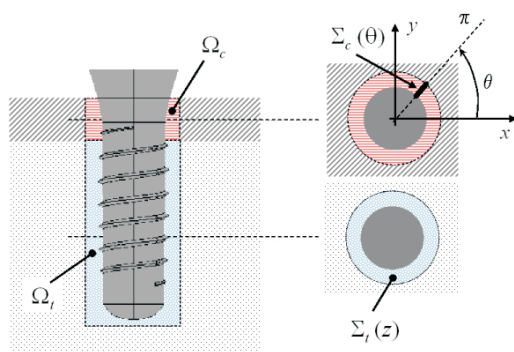


Fig. 5 Control regions employed to define local stress measures at the bone–implant interfacial region.

let $\Sigma_c(\theta)$ be the two-dimensional region resulting from the intersection between Ω_c and a plane π through the implant axis and identified by the angle θ with respect to the buccal–lingual axis (x in Fig. 4).

Accordingly, the following Von Mises (σ_v) and principal (σ_C , σ_T) stress measures can be introduced

$$\sigma_v^b(\delta) = \frac{1}{\mathcal{D}(\delta)} \int_{\mathcal{D}(\delta)} \sigma_{VM}(x, y, z) da \quad (1)$$

$$\sigma_T^b(\delta) = \max_{\mathcal{D}(\delta), i=1,2,3} \{\sigma_i(x, y, z), 0\} \quad (2)$$

$$\sigma_C^b(\delta) = \min_{\mathcal{D}(\delta), i=1,2,3} \{\sigma_i(x, y, z), 0\} \quad (3)$$

where the domain $\mathcal{D}(\delta)$ is $\Sigma_t(z)$ for stress measures relevant to the trabecular peri-implant region ($\delta = z$, $b = t$) and $\Sigma_c(\theta)$ for those defined at the compact bone ($\delta = \theta$, $b = c$).

It is worth observing that σ_v gives a measure of the local mean stress distribution at the implant–bone interface, whereas σ_T and σ_C furnish overloading risk measures at the peri-implant regions with reference to tensile and compressive states, respectively.

The previously introduced stress measures are numerically computed through a post-processing phase performed by means of a homemade MatLab–procedure, taking as input by the solver code some primary geometrical and topological data (i.e. nodal coordinates and elements which lies at the bone–implant interfacial regions Ω_t and Ω_c) as well as stress solutions at the integration points.

3 Results and discussion

3.1 Single-tooth commercial dental implants

Figures 6 and 7 show Von Mises stress distributions relevant to the five commercial endosteal implant here investigated. In detail, with reference to a mesial–distal cross–section view, stress contours on both maxillary and mandibular bone segments are put in comparison. In order to allow a significant analysis at compact and trabecular peri-implant regions, two different contour legends are used.

Proposed numerical results clearly highlight that the load transmission mechanisms strongly depend on the implant shape as well as on the healed compact bone geometry at the peri-implant region, that is on the type of crestal bone loss.

In detail, stress values on cortical bone seem to be essentially affected by the maximum diameter d of the implant, despite of the bone–implant interface length ℓ . Nevertheless, a reduction of stress concentrations on cancellous bone is obtained when ℓ increases for a given d . Moreover, although implants Branemark 1 and Ankylos have comparable values of d , the cortical bone shape around the Ankylos device yields lower stress values.

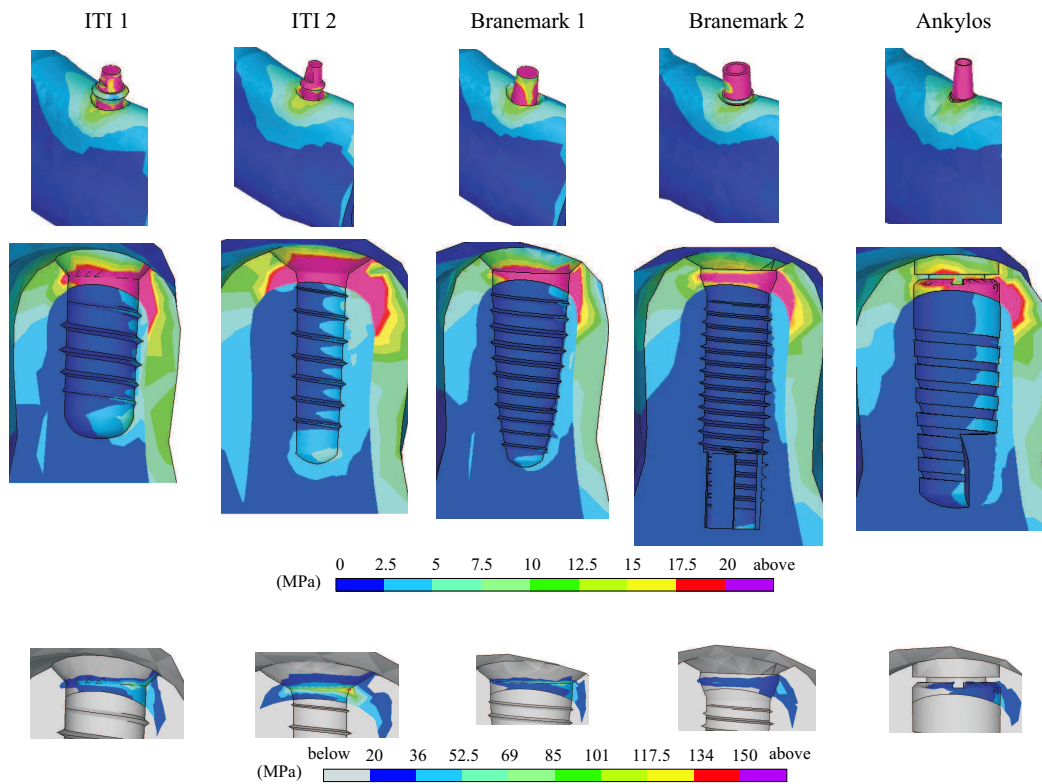


Fig. 6 Von Mises stress contours at the mesial–distal section–view (i.e., at $y = 0$) for single–tooth commercial endosteal implants in molar mandibular segment.

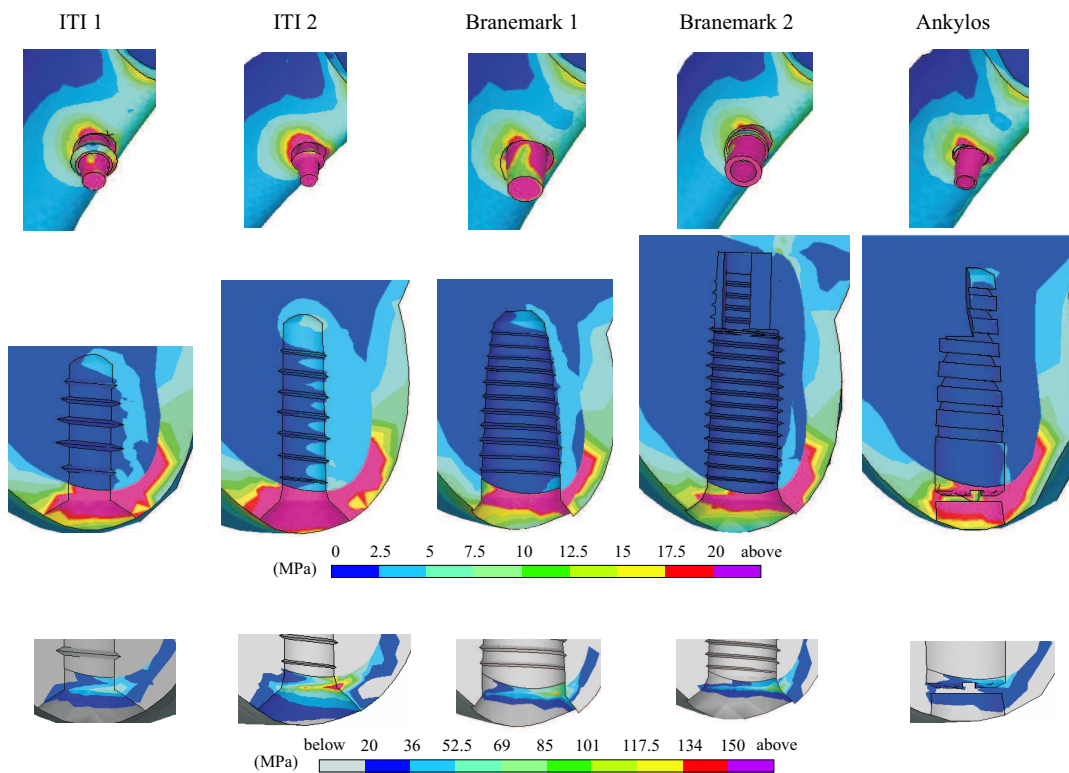


Fig. 7 Von Mises stress contours at the mesial–distal section–view (i.e., at $y = 0$) for single–tooth commercial endosteal implants in molar maxillary segment.

These considerations are fully confirmed by the analysis of Fig. 8, which depicts the values of the principal and Von Mises stress measures at the bone–implant interface (cortical and trabecular) and relevant to insertions in both mandibular and maxillary molar segments.

Proposed results highlight that the highest values at the compact bone of Von Mises and compressive stresses arise in the maxillary segment and they are deeply affected on implant shape. Moreover, tensile peaks are significantly smaller than compressive ones and their values seems to be fairly dependent on implant geometry.

Quantitative stress analysis highlights that the previously–introduced compressive physiological limits [50, 51] are exceeded when the implants ITI 1, ITI 2 and Branemark 2 are experienced on the maxillary segment, whereas tensile bone strength is never reached.

Ankylos implant exhibits the best performance on the cortical bone interface, for both mandibular and maxillary placements. It induces the lowest compressive and tensile stress values, producing at the same time fully acceptable stresses at the cancellous bone interface. On the other hand, the worst load transfer mechanisms are computed on the mandibular (maxillary) segment considering the implants Branemark 1 and ITI 2 (ITI 2). In detail, average stress values in mandibular cortical bone and relevant to the implants Branemark 1 overcome of about 140% in tension and 290% in compression (180% considering the Von Mises stress measure) those of the Ankylos system. Moreover, when an implant ITI 2 is used, stress values in maxillary cortical bone are much greater (about 150% in tension, 600% in compression, 300% for the Von Mises measure) than those obtained in the case of the Ankylos implant. As far as principal stresses at cancellous bone are concerned, tensile peaks are always greater than compressive ones and significant concentrations can appear at the trabecular–compact bone interface as well as, with smaller values, at the bottom region of the screw. These concentrations exceed the strength of the cancellous bone (about 5 MPa in tension and compression [50]) for all the investigated implants, except that for the Ankylos system.

3.2 Double–implant with a retaining bar

Figure 9 shows Von Mises stress distributions relevant to numerical analyses performed on the DIRB device inserted in a mandibular bone segment and relevant to three different locations of the occlusal force: at the middle of the retaining bar (case A in figure) and in correspondence of the mesial (B) and distal (C) Ankylos implants.

Table 3 summarizes maximum values of Von Mises and principal stress measures, computed at trabecular and compact peri–implant regions.

It is worth observing that tensile and compressive stress peaks are comparable for the three cases under investigation, for both cancellous and compact bone. On the other hand, the highest Von Mises stress values com-

puted for mesial and distal loading conditions are substantially twice than in the case of the middle–located force. Nevertheless, it clearly appears that tensile and compressive physiological limits are practically never exceeded, resulting in a good mechanical performance of this Ankylos–based multi–implant device.

Tab. 3 Maximum values (in MPa) of Von Mises (σ_v) and principal (σ_C , σ_T) stress measures computed at the trabecular (σ^t) and compact (σ^c) peri–implant regions (mesial and distal) for the DIRB device. Load locations are identified in agreement with the notation introduced in Fig. 4.

risk measures	load position					
	mesial implant			distal implant		
	A	B	C	A	B	C
$(\sigma_v^c)_{\max}$	18.3	29.5	8.8	19.7	7.3	27.3
$(\sigma_v^t)_{\max}$	1.1	2.3	0.7	1.0	0.5	1.7
$ \sigma_C^c _{\max}$	18.6	22.8	8.4	20.5	7.7	28.3
$ \sigma_C^t _{\max}$	2.2	5.1	1.1	2.0	1.0	4.0
$(\sigma_T^c)_{\max}$	9.5	14.8	3.8	8.6	5.9	16.2
$(\sigma_T^t)_{\max}$	3.0	4.7	1.1	2.6	1.1	4.5

3.3 Non conventional mini–implant applications

Figure 10 depicts Von Mises stress distributions relevant to mini–implant devices (MI) inserted in a mandibular bone segment. As discussed in the section 2.1, two mini–screws dispositions (vertical -MI₀- and angled -MI₂₅-, see Fig. 3) are analyzed.

Table 4 summarizes maximum values of Von Mises and principal stress measures, experienced at the trabecular and compact peri–implant regions.

It can be noted that the highest values of Von Mises and principal stress measures are computed in the case of the angled device (MI₂₅). In detail, compressive and tensile stress measures relevant to the case MI₂₅ result greater than those experienced for MI₀ of about 90%. Moreover, cortical physiological limits are slightly exceeded only in tension for the MI₂₅ device, whereas trabecular limits are exceeded in both MI cases.

Nevertheless, proposed results show that MI devices exhibit a fully comparable or even better mechanical behaviour than some standard commercial single–tooth implants, such as Branemark or ITI ones analyzed in this study. Furthermore, implant systems based on mini–screws should offer long–term stability advantages.

4 Concluding remarks

In this paper five commercial endosteal dental implants (two ITI implants, two Nobel Biocare and an Ankylos one) and a number of multiple–implant applications (a double–implant system based on a retaining bar -DIRB- for a triple–teeth restoration and non–conventional single–tooth devices -MI- based on en-

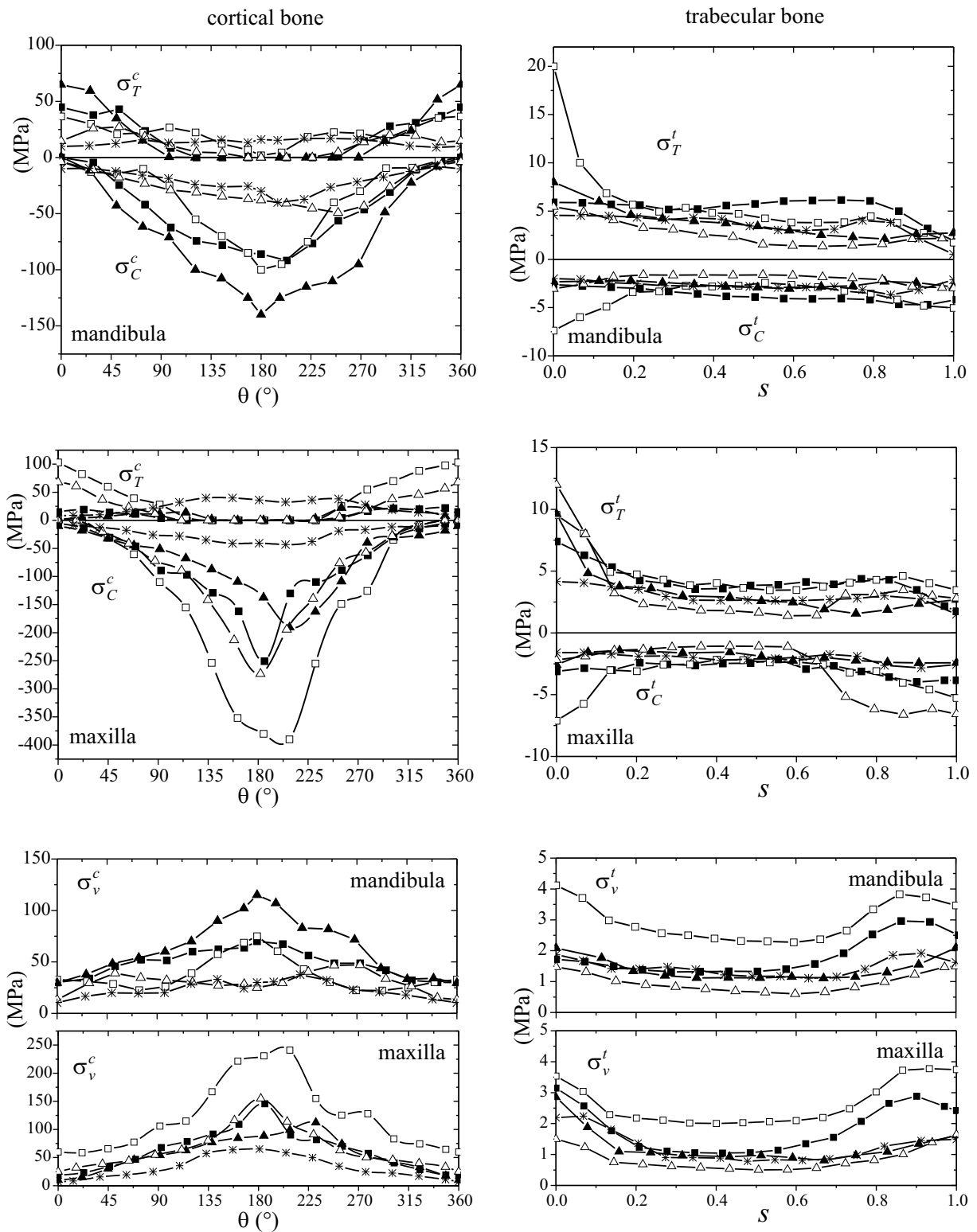


Fig. 8 Von Mises (σ_v) and principal (σ_C , σ_T) stress measures computed at the compact (σ^c , on the left) and trabecular (σ^t , on the right) peri-implant interface for mandibular and maxillary insertions. s denotes the dimensionless abscissa along the implant axis, such that $s = 0$ at the cortical-trabecular bone interface and $s = 1$ at the inserted implant end. —■— ITI 1; —□— ITI 2; —△— Branemark 1; —▲— Branemark 2; —*— Ankylosis.

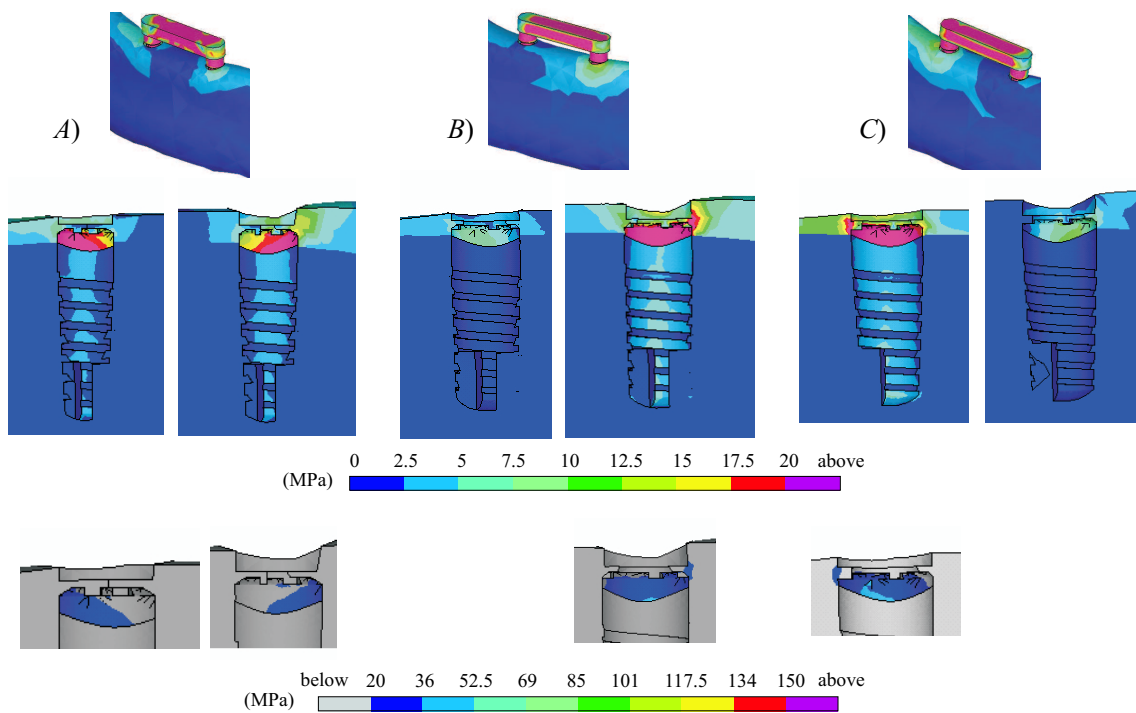


Fig. 9 Von Mises stress contours at the mesial–distal section–view (i.e., at $y = 0$) for the DIRB application and considering different load locations: A) at the middle of the retaining bar; B) at the mesial implant; C) at the distal implant.

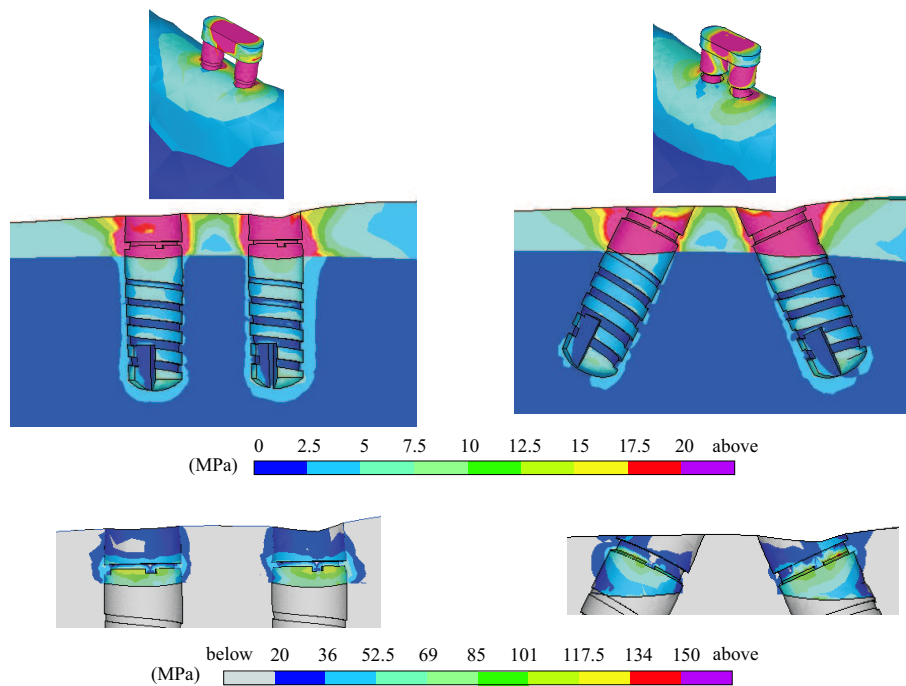


Fig. 10 Von Mises stress contours at the mesial–distal section–view (i.e., at $y = 0$) for mini–implant applications: MI₀ on the left and MI₂₅ on the right.

Tab. 4 Maximum values (in MPa) of Von Mises (σ_v) and principal (σ_C , σ_T) stress measures computed at the trabecular (σ^t) and compact (σ^c) peri-implant regions (around mesial and distal Ankylos-type mini-screws) for MI devices (see Fig. 2).

risk measures	mini-screw disposition			
	mesial implant		distal implant	
	MI ₀	MI ₂₅	MI ₀	MI ₂₅
$(\sigma_v^c)_{\max}$	94.3	62.5	101.8	47.2
$(\sigma_v^t)_{\max}$	4.9	8.2	4.8	3.1
$ \sigma_C^c _{\max}$	91.3	165.9	83.9	161.0
$ \sigma_C^t _{\max}$	15.3	8.0	7.6	5.2
$(\sigma_T^c)_{\max}$	52.9	91.6	52.6	193.7
$(\sigma_T^t)_{\max}$	12.1	8.3	13.2	9.1

osseous mini-screws) were numerically investigated by means of static linearly elastic three-dimensional finite-element analyses, under functional loading conditions and considering insertions in both mandibular and maxillary molar bone segments.

Three-dimensional numerical models were built-up employing CAT images and comparative techniques. Complete osseous integration and different quality of trabecular bone were taken into account for the mandibular and maxillary regions. Moreover, depending on the crestal bone loss induced by implant shape, different compact bone geometries around the implant neck were modelled. In order to analyze the influence of the implant shape and the risk of bone weakening or loss due to local tissue overloading, a stress analysis was performed, both in terms of global and local (at the bone-implant interface) stress measures.

The five osseointegrated implants exhibit deeply different mechanical behaviour, depending on their shape parameters and on the site of placement. In detail, the worst performance on the maxillary bone was observed for the implant ITI 2, whereas on the mandibular segment for Branemark 1 and ITI 2. On the contrary, the best load transmission mechanisms appeared considering the Ankylos system. An efficient performance on both cancellous and compact bone, comparable with the Ankylos' implant, was numerically experienced for the Branemark 2 implant when mandibular placement was considered. Nevertheless, Branemark 2 exhibited significant compressive stress peaks on maxillary compact bone segment, such as implants ITI 1 and ITI 2.

Proposed results highlight that, under a given occlusal force, load transmission mechanisms of osseointegrated implants are strongly dependent on the maximum diameter of the screw and on the length of the bone-implant interface, as well as on the site of placement. Moreover, present numerical analyses show that compressive and tensile stresses relevant to maxillary systems are generally greater than mandibular ones, both in cortical and cancellous bone, inducing an higher implant fail-

ure risk, in accordance with well-established clinical experiences. Numerical results show also that possible overloading at compact bone occurs in compression whereas, at the interface between cortical and trabecular bone, overloading can occur in tension.

Analysis of the DIRB system shows the effectiveness of this device when Ankylos implants are employed. As a matter of fact, quantitative stress analysis relevant to different loading locations upon the retaining bar highlights that compressive and tensile bone physiological limits are not exceeded.

On the other hand, overloading states appear in single-tooth mini-implant applications (MI) based on two Ankylos-type mini-screws. Nevertheless, their load transmission mechanisms are fully comparable with a number of conventional single-tooth implants (such as Branemark or ITI ones). Accordingly, MI systems can be considered a real alternative to traditional single-tooth implants, when geometrical configuration of the site of insertion and bone quantity and quality (particularly in sinus zone) do not allow to employ a single greater screw. Moreover, mini-implant devices should allow more effective long-term stability results, especially experiencing an angled mini-screws configuration.

Acknowledgements

This work was developed within the framework of Lagrange Laboratory, an European research group comprising CNRS, CNR, the Universities of Rome "Tor Vergata", Calabria, Cassino, Pavia, and Salerno, Ecole Polytechnique, University of Montpellier II, ENPC, LCPC, and ENTPE.

5 References

- [1] R.J. Weyant. Short-term clinical success of root-form titanium implant systems. *The Journal of Evidence-Based Dental Practice*, 3(3):127-130, 2003.
- [2] A.M. Roos-Jansåker, C. Lindahl, H. Renvert and S. Renvert. Nine- to fourteen-year follow-up of implant treatment. Part I: implant loss and associations to various factors. *Journal Of Clinical Periodontology*, 33(4):283-289, 2006.
- [3] A. Piattelli, A. Scarano and M. Piattelli. Microscopic aspects of failure in osseointegrated dental implants: a report of five cases. *Biomaterials*, 17(12):1235-1241, 1996.
- [4] A.N. Natali and P.G. Pavan. Numerical approach to dental biomechanics. *Dental Biomechanics*. In Natali A.N., editor, London: Taylor & Francis, p. 211-39, 2003.
- [5] A.N. Natali and P.G. Pavan. A comparative analysis based on different strength criteria for evaluation of risk factor for dental implants. *Computer Methods in Biomechanics and Biomedical Engineering*, 5(1):511-23, 2002.

- [6] D.L. Cochran. A comparison of endosseous dental implant surfaces. *Journal of Periodontology*, 70(12):1523–39, 1999.
- [7] D. Siegele and U. Soltesz. Numerical investigations of the influence of implant shape on stress distribution in the jaw bone. *International Journal of Oral and Maxillofacial Implants*, 4(4):333–40, 1989.
- [8] H.J. Chun, S.Y. Cheong, J.H. Han, S.J. Heo et al. Evaluation of design parameters of osseointegrated dental implants using finite element analysis. *Journal of Oral Rehabilitation*, 29: 565–74, 2002.
- [9] M. Soncini, R. Rodriguez y Baena, R. Pietrabissa, V. Quaglini, S. Rizzo and D. Zaffe. Experimental procedure for the evaluation of the mechanical properties of bone surrounding dental implants. *Biomaterials*, 23:9–17, 2002.
- [10] C.M. Stanford and G.B. Schneider. Functional behaviour of bone around dental implants. *Gerodontology*, 21:71–7, 2004.
- [11] L. Chun–Li, C. Shih–Hao and W. Jen Chyan. Finite element analysis of biomechanical interactions of tooth–implant splinting system for various bone qualities. *Chang Gung Medical Journal* 29:143–53, 2006.
- [12] Saime Şahin, Murat C. Çehreli and Emine Yaşın. The influence of functional forces on the biomechanics of implant–supported prostheses—a review. *Journal of Dentistry*, 30:71–82, 2002.
- [13] E. Chaichanasiri, P. Nanakorn, W. Tharanon and J.V. Sloten. A numerical study of bone stress distributions around dental implant: influence of adjacent teeth. *ISBME 2006, 2nd International Symposium on Biomedical Engineering*, Bangkok, Thailand.
- [14] T. Jemt, J. Chai, J. Harnett, M.R. Heath, J.E. Hutton, R.B. Johns et al. A 5-year prospective multicenter follow-up report on overdentures supported by osseointegrated implants. *International Journal of Oral and Maxillofacial Implants*, 11:291–8, 1996.
- [15] S.E. Eckert and P.C. Wollan. Retrospective review of 1170 endosseous implants placed in partially edentulous jaws. *Journal of Prosthetic Dentistry*, 79:415–21, 1998.
- [16] U. Lekholm, J. Gunne, P. Henry, K. Higuchi, U. Linden, C. Bergstrom et al. Survival of the Branemark implant in partially edentulous jaws: a 10–year prospective multicenter study. *International Journal of Oral and Maxillofacial Implants*, 14:639–45, 1999.
- [17] C.E. Misch and M.W. Bidez. A scientific rationale for dental implant design. *Contemporary implant dentistry* Misch CE, editor. 2nd ed., St. Louis: Mosby, p. 329–43, 1999.
- [18] E. Fernandez, F.J. Gil, C. Aparicio, M. Nilsson, S. Sarda, D. Rodriguez, et al. Material in dental implantology. *Dental Biomechanics* Natali A.N., editor, London: Taylor & Francis, p. 69–89, 2003.
- [19] O.C. Zienkiewicz and R.L. Taylor. *The Finite Element Method*. 4th ed. New York: McGraw-Hill, 1998.
- [20] S. Joshi, A. Mukherjee, M. Kheur and A. Metha. Mechanical performance of endodontically treated teeth. *Finite Elements in Analysis and Design*, 37:587–601, 2001.
- [21] P. Ausiello, A. Apicella and C.L. Davidson. Effect of adhesive layer properties on stress distribution in composite restorations: a 3D finite element analysis. *Dental Materials*, 18: 295–303, 2002.
- [22] E. Asmussen, A. Peutzfeldt and A. Sahafi. Finite element analysis of stresses in endodontically treated, dowel-restored teeth. *Journal of Prosthetic Dentistry*, 94: 321–9, 2005.
- [23] F. Maceri, M. Martignoni and G. Vairo. Mechanical behaviour of endodontic restorations with multiple prefabricated posts: A finite element approach. *Journal of Biomechanics*, 40(11): 2386–98, 2007.
- [24] I.P. Geng, K.B. Tan and G.R. Liu. Application of finite element analysis in implant dentistry: a review of the literature. *Journal of Prosthetic Dentistry*, 85:585–98, 2001.
- [25] R.C. Van Staden, H. Guan and Y.C. Loo. Application of the finite element method in dental implant research. *Computer Methods in Biomechanics and Biomedical Engineering*, 9(4):257–70, 2006.
- [26] M.R. Rieger, W.K. Adams and G.L. Kinzel. A finite element survey of eleven endosseous implants. *Journal of Prosthetic Dentistry*, 63:457–65, 1990.
- [27] C.S. Petrie and J.L. Williams. Comparative evaluation of implant designs: influence of diameter, length, and taper on strains in the alveolar crest. A three-dimensional finite-element analysis. *Clinical Oral Implants Research*, 16(4):486–94, 2005.
- [28] E.P. Holmgren, R.J. Seckinger, L.M. Kilgren and F. Mante. Evaluating parameters of osseointegrated dental implants using finite element analysis—a two dimensional comparative study examining the effects of implant diameter, implant shape, and load direction. *Journal of Oral Implantology*, 24:80–8, 1998.
- [29] L. Zhiyong, T. Arataki, I. Shimamura and M. Kishi. The influence of prosthesis designs and loading conditions on the stress distribution of tooth-implant supported prostheses. *Bulletin of Tokyo Dental College*, 45(4):213–21, 2004.
- [30] D. Bozkaya, S. Muftu and A. Muftu. Evaluation of load transfer characteristics of five different implants in compact bone at different load levels by finite elements analysis. *Journal of Prosthetic Dentistry*, 92(6):523–30, 2004.
- [31] H.J. Chun, H.S. Shin, C.H. Han and S.H. Lee. Influence of implant abutment type on stress distribution in bone under various loading conditions using finite element analysis. *International Journal of Oral Maxillofacial Implants*, 21(2):195–202, 2006.

- [32] T. Kitagawa, Y. Tanimoto, K. Nemoto and M. Aida. Influence of cortical bone quality on stress distribution in bone around dental implant. *Dental Materials Journal*, 24(2):219-24, 2005.
- [33] X.E. Saab, J.A. Griggs, J.M. Powers and R.L. Engelmeier. Effect of abutment angulation on the strain on the bone around an implant in the anterior maxilla: a finite element study. *Journal of Prosthetic Dentistry*, 97(2):85-92, 2007.
- [34] H.J. Chun, D.N. Park, C.H. Han, S.J. Heo, M.S. Heo and J.Y. Koak. Stress distributions in maxillary bone surrounding dental implants with different overdenture attachments. *Journal of Oral Rehabilitation*, 32:193-205, 2005.
- [35] A.N. Natali, P.G. Pavan and A.L. Ruggero. Evaluation of stress induced in peri-implant bone tissue by misfit in multi-implant prosthesis. *Dental Materials*, 22(4):388-95, 2006.
- [36] D.P. Callan, A. O'Mahony and C.M. Cobb. Loss of crestal bone around dental implants: a retrospective study. *Implant Dentistry*, 7(4):258-66, 1998.
- [37] Y.K. Shin, C.H. Han, S.J. Heo, S. Kim and H.J. Chun. Radiographic evaluation of marginal bone level around implants with different neck designs after 1 year. *International Journal of Oral Maxillofacial Implants*, 21(5):789-94, 2006.
- [38] C.M. Becker and D.A. Kaiser. Implant-retained cantilever fixed prosthesis: Where and when. *Journal of Prosthetic Dentistry*, 84:432-5, 2000.
- [39] M.A. Papadopoulos and F. Tarawneh. The use of miniscrew implants for temporary skeletal anchorage in orthodontics: A comprehensive review. *Oral Surgery, Oral Medicine, Oral Pathology, Oral Radiology and Endodontics*, 103:e6-15, 2007.
- [40] H.L. Huang, J.S. Huang, C.C. Ko, J.T. Hsu, C.H. Chang, M.Y.C. Chen. Effect of splinted prosthesis supported a wide implant or two implants: a three-dimensional finite element analysis. *Clinical Oral Implants Research* 16:466-72, 2005.
- [41] K. Arkça and H. İplikçioğlu. Comparative evaluation of the effect of diameter, length and number of implants supporting three-unit fixed partial prostheses on stress distribution in bone. *Journal of Dentistry*, 30:40-6, 2002.
- [42] J. Mah and F. Bergstrand. Temporary anchorage devices: a status report. *Journal of Clinical Orthodontics*, 39:132-6, 2005.
- [43] M. Dalstra, P.M. Cattaneo and B. Melsen. Load transfer of miniscrews for orthodontic anchorage. *Orthodontics*, 1:53-62, 2004.
- [44] J.W. Lim, W.S. Kim, I.K. Kim, C.Y. Son and H.I. Byun. Three dimensional finite element method for stress distribution on the length and diameter of orthodontic miniscrew and cortical bone thickness. *Korean Journal of Orthodontics*, 33:11-20, 2003.
- [45] H.M. Kyung, H.S. Park, S.M. Bae, J.H. Sung and I.B. Kim. Development of orthodontic microimplants for intraoral anchorage. *Journal of Clinical Orthodontics*, 37:321-8, 2003.
- [46] J.E. Lemon and F. Dietsh-Misch. Biomaterials for dental implants. In Misch CE, editor, *Contemporary implant dentistry*, 2nd ed. St. Louis: Mosby, p. 271-302, 1999.
- [47] U. Lekholm and G.A. Zarb. Patient selection and preparation. In P.I. Branemark, G.A. Zarb, T. Albrektsson, editors, *Tissue-integrated prostheses: osseointegration in clinical dentistry*, Chicago: Quintessence, p. 199-209, 1985.
- [48] A.N. Natali, P.G. Pavan and A.L. Ruggero. Evaluation of stress induced in peri-implant bone tissue by misfit in multi-implant prosthesis. *Dental Materials*, 22:388-95, 2006.
- [49] H. Van Oosterwyck, J. Duyck, J. Vander Sloten, G. Van der Perre, M. De Cooman, S. Lievens et al. The influence of bone mechanical properties and implant fixation upon bone loading around oral implants. *Clinical Oral Implants Research*, 9: 4017-18, 1998.
- [50] R.B. Martin, D.B. Burr and N.A. Sharkey. *Skeletal tissue mechanics*. 1st ed. Springer, New York, 1998.
- [51] A.N. Natali, R.T. Hart, P.G. Pavan and I. Knets. Mechanics of bone tissue. *Dental Biomechanics*. In Natali A.N., editor. London: Taylor & Francis, p. 1-19, 2003.